Differential Activities of DNA Polymerases in Processing Ribonucleotides during DNA Synthesis in Archaea

Mélanie Lemor, Ziqing Kong, Etienne Henry, Raphaël Brizard, Sébastien Laurent, Audrey Bossé, Ghislaine Henneke

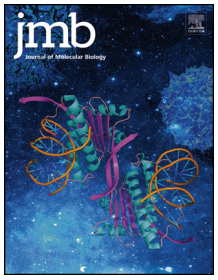

Differential Activities of DNA Polymerases in Processing Ribonucleotides during DNA Synthesis in *Archaea*

Mélanie Lemor [1], Ziqing Kong [2], Etienne Henry [3], Raphaël Brizard [1], Sébastien Laurent [1], Audrey Bossé [1] and Ghislaine Henneke [1]

1 - Ifremer, *Univ Brest, CNRS, Laboratoire de Microbiologie des Environnements Extrêmes, F-29280 Plouzané, France*
2 - Department of Medical Biochemistry and Biophysics, *Umeå University, Umeå, Sweden*
3 - CNRS, *Ifremer, Univ Brest, Laboratoire de Microbiologie des Environnements Extrêmes, F-29280, Plouzané, France*

Correspondence to Ghislaine Henneke: *Ghislaine.Henneke@ifremer.fr*
https://doi.org/10.1016/j.jmb.2018.10.004
Edited by M Gottesman

Abstract

Consistent with the fact that ribonucleotides (rNTPs) are in excess over deoxyribonucleotides (dNTPs) *in vivo*, recent findings indicate that replicative DNA polymerases (DNA Pols) are able to insert ribonucleotides (rNMPs) during DNA synthesis, raising crucial questions about the fidelity of DNA replication in both *Bacteria* and *Eukarya*. Here, we report that the level of rNTPs is 20-fold higher than that of dNTPs in *Pyrococcus abyssi* cells. Using dNTP and rNTP concentrations present *in vivo*, we recorded rNMP incorporation in a template-specific manner during *in vitro* synthesis, with the family-D DNA Pol (PolD) having the highest propensity compared with the family-B DNA Pol and the p41/p46 complex. We also showed that ribonucleotides accumulate at a relatively high frequency in the genome of wild-type *Thermococcales* cells, and this frequency significantly increases upon deletion of RNase HII, the major enzyme responsible for the removal of RNA from DNA. Because ribonucleotides remain in genomic DNA, we then analyzed the effects on polymerization activities by the three DNA Pols. Depending on the identity of the base and the sequence context, all three DNA Pols bypass rNMP-containing DNA templates with variable efficiency and nucleotide (mis)incorporation ability. Unexpectedly, we found that PolD correctly base-paired a single ribonucleotide opposite rNMP-containing DNA templates. An evolutionary scenario is discussed concerning rNMP incorporation into DNA and genome stability.

Introduction

Maintenance of genome integrity is essential for life, and faithful DNA replication and repair ensure this. One of the most important parameters for DNA maintenance is the regulation of optimal concentrations of the four 5′-deoxyribonucleoside-triphosphates (dNTPs) the precursors for DNA synthesis, by ribonucleotide reductase (RNR) [1]. RNR, which reduces the 5′-ribonucleoside-triphosphates (rNTPs) to the corresponding dNTPs, also maintains the ratio of rNTPs to dNTPs at distinct levels throughout the cell cycle. Moreover, the relative abundance of nucleotides is dependent on the type of tissue, organelle and cell, with rNTP content significantly exceeding dNTP content [2–4]. For these reasons, high- and low-fidelity DNA polymerases (DNA Pols) face the challenge of selecting the correct dNTPs over the more abundant rNTPs during the normal processes of DNA replication and repair. While cellular concentrations of these nucleotides are documented in *Eukarya* and *Bacteria*, they remain largely unknown in *Archaea* [5].

Other important parameters such as DNA Pol selectivity, proofreading 3′ → 5′ exonuclease activity and mismatch repair (MMR) contribute to improving the fidelity of DNA synthesis [6,7]. With regard to rNMP incorporation, high- and low-fidelity DNA Pols have evolved structural features for blocking rNTP entry into their active sites. A steric gate residue or a protein backbone segment is believed to generate a clash with the 2′-hydroxyl group of the ribose of the incoming rNTP [8]. This prevention mechanism is of

particular importance for the proofreading function of high-fidelity (HiFi) DNA Pols since it is more proficient in the excision of incorrect dNMPs than rNMPs from extending primers [9,10].

Recent data indicate that rNMPs are the main non-canonical nucleotides incorporated into DNA [11] by eukaryotic and bacterial DNA Pols, with surprisingly high frequency [2,12]. rNMP incorporation may also arise from imperfect processing of Okazaki fragments [13]. The biological evidence of embedded rNMPs in the DNA of *Bacteria*, *Archaea* and *Eukarya* is based on *in vivo* studies showing an increased load of genomic rNMPs and genetic instability in ribonuclease H (RNase H)-defective cells [11,14–17]. Because of the reactive 2′-hydroxyl group on the ribose ring, rNMPs in the chromosome make the DNA strand susceptible to spontaneous and enzymatic hydrolytic cleavage. They can also modify the helical structure in DNA that possibly interferes with cellular DNA transactions [18]. To prevent persistent rNMP accumulation in genomic DNA, cells evolved a specific repair pathway termed ribonucleotide excision repair (RER), in which the principal enzyme is type 2 RNase H (RNase H2 or HII) [14,19,20]. In the absence of RNase H2, a topoisomerase 1 (Top1 or topA gene) repair pathway can remove some rNMPs in yeast [21,22]. Moreover, rNMPs might also be targeted by other mechanisms such as MisMatch Repair (MMR), nucleotide excision repair (NER) and base excision repair (BER) [23–26].

Here, we sought to analyze whether rNMP incorporation into DNA is a conserved property of DNA synthesis in *Archaea*. Up to now, four DNA Pol families, (B, D, X and Y) and the p41/p46 primase–polymerase have been found in the genomes of 251 archaeal species (https://gold.jgi.doe.gov/). *In vitro* activities of families B, D and Y and the p41/p46 complex of archaeal DNA Pols have been demonstrated, but never characterized for the X-family. Which DNA Pols are responsible for duplicating the archaeal genome is not currently known with the same degree of certainty as for *Bacteria* or *Eukarya*. All *Archaea* contain a family-B DNA Pol (PolB), usually present as several members in the Crenarchaea and as a single enzyme in the Euryarchaea. With the exception of the Crenarchaea, a HiFi family-D DNA Pol (PolD) is found in all *Archaea* and is unique to this domain. *Archaea* also possess a p41/p46 primase–polymerase complex with p41 belonging to archaeo-eukaryotic primase (AEP) family. At the replication fork in the Crenarchaea, it is believed that the p41/p46 complex initiates DNA replication by synthesizing an RNA primer, followed by leading and lagging strand DNA synthesis using HiFi family-B DNA Pols [27–29]. While it is clear that p41/p46 is involved in the initiation process in the Euryarchaea [30–32], the role of HiFi PolB and/or PolD acting selectively on opposite DNA strands at the replication fork remains inconclusive because of biochemical and genetic divergences [33–39]. Similar to the DNA repair family-Y DNA Pol [28,40,41], it is not excluded that the p41/p46 complex, like families B and D DNA Pols, might operate in other archaeal DNA transactions (repair, damage tolerance, damage signaling, *etc.*) [14,27,31,33,42–46].

In the present work, we ask whether rNMP incorporation is an evolutionarily conserved property of DNA synthesis in *Archaea*. For this purpose, we used the best characterized hyperthermophilic anaerobe, *Pyrococcus abyssi* GE5 [47]. This strain duplicates its genome as fast as *Bacteria*, supported by eukaryotic-like replication proteins [48]. Roles have been proposed whereby RNA priming is performed by the p41/p46 complex [31], followed by leading and lagging strand DNA synthesis by PolB and PolD, respectively [35,49,50],. Maturation of Okazaki fragments likely involves PolD but precludes any contribution of PolB in the absence of RNase HII [34]. Beyond these crucial roles in DNA replication, all three DNA polymerizing enzymes seem to work in DNA transactions such as repair, damage signaling or tolerance [31,42,43,51]. We further analyzed whether rNMP incorporation by PolB, PolD and the p41/p46 complex is conserved during DNA synthesis. At the physiological dNTP and rNTP levels, we demonstrate that PolD is the main DNA Pol able to insert rNMPs in an error-free manner. In addition, we report that single embedded rNMPs are bypassed by all three DNA Pols with variable nucleotide incorporation/misincorporation proficiency regardless of the nature of the base and sequence context. Unexpectedly, we also discovered that PolD can incorporate a single rNMP opposite template ribonucleotides. These results suggest that rNMP incorporation into DNA represents a conserved feature of archaeal DNA Pols, which may have various consequences for their genome integrity.

Results

dNTP and rNTP pools in *P. abyssi*

We first measured the levels of dNTPs and rNTPs in exponentially growing *P. abyssi* cells (Table 1).

Table 1. Intracellular levels of nucleotides in exponentially growing *P. abyssi* cells

dNTPs	Concentration (pmol/10^8 cells)	rNTPs	Concentration (pmol/10^8 cells)
dA	8.1 ± 3.8	rA	288.0 ± 93.1
dC	2.8 ± 1.5	rC	84.1 ± 25.6
dG	8.8 ± 4.2	rG	185.0 ± 41.7
dT	17.1 ± 7.2	rU	162.0 ± 46.0

The levels of dNTPs and rNTPs were evaluated from exponentially growing cells. The nucleotide pool represents the average of 14 and 15 replicate experiments from three different biological samples. Mean ± standard deviation values are shown.

The results demonstrate that rNTP content is 20-fold higher than dNTP content and corroborate previous data showing that rNTP concentrations are 10- to 80-fold higher than those of dNTPs in *Escherichia coli* and *Saccharomyces cerevisiae* cells [2,3], respectively. Thus, amounts of rNTPs in our hyperthermophilic anaerobe archaeal cells significantly exceed those of dNTPs, and values range from 288 pmol/10^8 cells for rATP to 2.8 pmol/10^8 cells for dCTP (Table 1).The rNTP/dNTP ratios vary from 35/1 for adenine and 10/1 for ribouridine/deoxythymidine. Moreover, the relative quantities of dNTPs (dT > dG ≥ dA > dC) differ from those of rNTPs (rA > rG ≥ rU > rC).

Influence of nucleotide pools on primer extension activities

To study the effects of rNTP and dNTP levels on DNA synthesis, primer extension reactions were carried out in the presence of individual DNA Pols (PolD, PolB and the p41/p46 complex) from *P. abyssi*. Two concentrations of nucleotides (ratios 1 and 2) were used according to the cellular rNTP/dNTP ratios (Table 1). The reference for calculating the balance with the seven remaining nucleotides in ratio 1 was 200 μM of dTTP, resembling that believed to usually occur in *Bacteria* and *Eukarya* [2,3]. The rNTP reference for calculating the balance with the seven remaining nucleotides in ratio 2 was 200 μM of rATP. The basal references of these two ratios were used throughout this study because they correspond to previous working nucleotide concentrations (200 μM of either dNTPs or rNTPs) supplied to *P. abyssi* DNA Pols in extension assays [31,35].

Primer extension reactions with 200 μM of the four dNTPs were examined in the presence of individual DNA Pols (Fig. 1b–d, lane 3). The results showed that extension of the DNA primer was highly efficient for the three DNA Pols (more than 90% extension)

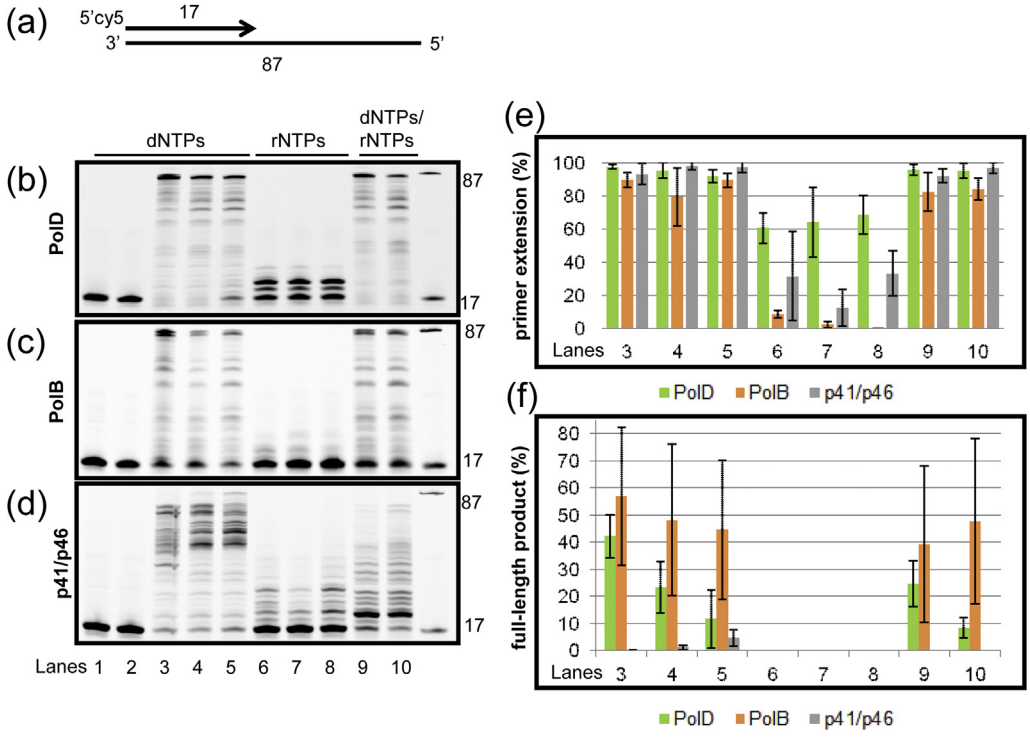

Fig. 1. Influence of nucleotide pools on primer extension activities. (a) Structure of the 5′-Cy5-labeled 17/87 primer-template (for full sequences, see Table S1). (b–d) Extension reactions using PolD (b), PolB (c) and the p41/p46 complex (d) from *P. abyssi* during a 30-min reaction containing the following: lane 1, control p/t without enzyme; lane 2, control without incubation; lane 3, all four dNTPs at 200 μM each; lane 4, ratio 1 with all four dNTPs at 95 μM dATP, 103 μM dGTP, 200 μM dTTP and 33 μM dCTP; lane 5, ratio 2 with all four dNTPs at 5.6 μM dATP, 6.1 μM dGTP, 11.9 μM dTTP and 2 μM dCTP; lane 6, all four rNTPs at 200 μM each; lane 7, ratio 1 with all four rNTPs at 3359 μM rATP, 2157 μM rGTP, 1889 μM rUTP and 981 μM rCTP; lane 8, ratio 2 with all four rNTPs at 200 μM rATP, 128.4 μM rGTP, 112.4 μM rUTP and 58.4 μM rCTP; lane 9, ratio 1 with all four dNTPs and rNTPs; lane 10, ratio 2 with all four dNTPs and rNTPs. Reference oligodeoxynucleotides of 87 and 17 bases are indicated on the right of each panel. Gel images of reaction products shown in panels b–d were quantified as described in Materials and Methods. Bar graphs of extension and full-length products are summarized in panels e and f, respectively. Bars represent the averages (±standard deviation) of at least three independent experiments.

(Fig. 1e, lane 3). Inspection of full-length extension products indicated that the p41/p46 complex was not very proficient in synthesis of long DNA fragments as compared with PolB and PolD (Fig. 1f, lane 3). Among the two HiFi DNA Pols, PolB was the most active. When dNTPs were used at the physiological ratios, almost identical profiles of polymerization were observed with PolD and PolB (Fig. 1b and c, lanes 4–5). In this case, extension of the DNA primer was comparable with that of 200 μM dNTPs (Fig. 1e, lane 3 compared with lanes 4–5) and a slight reduction of full-length product was observed (Fig. 1f, lane 3 compared with lanes 4–5). In contrast, the p41/p46 complex was much more sensitive to the balance and concentration of dNTPs (Fig. 1d, lane 3 compared with lanes 4–5). Decreasing the concentration of dNTPs (from ratio 1 to 2) resulted in the synthesis of longer DNA fragments by the p41/p46 complex (Fig. 1d and f, lanes 4–5). Taken together, these results show that the balance and concentration of dNTPs affect DNA synthesis more strongly by the p41/p46 complex than by the two HiFi DNA Pols.

When primer extension reactions were carried out with 200 μM of the four rNTPs in the presence of individual DNA Pols, the highest incorporation efficiency was observable with PolD (60% extension) (Fig. 1e, lane 6), extending from DNA primers as short as 4 rNMPs (Fig. 1b–d, lane 6). About 2-fold reduction of rNMP incorporation was obtained for the p41/p46 complex compared with PolD, while showing addition of at least 6 rNMPs from the DNA primer (Fig. 1d and e, lane 6). Comparatively, PolB did not retain significant DNA primer extension (Fig. 1c and e, lane 6). When rNTPs were used at the physiological ratios, almost identical profiles of polymerization were observed, with PolD and the p41/p46 complex being the most proficient at rNMP incorporation (Fig. 1b–d and e, lane 6 compared with lanes 7–8). In addition, the balance and concentration of rNTPs mainly affected the polymerization activity of the p41/p46 complex (Fig. 1d, lane 6 compared with lanes 7–8). In particular, a stimulation of rNMP incorporation is observed upon decreasing concentrations for the p41/p46 complex (Fig. 1e, lanes 7–8), while no major changes were seen with PolD (Fig. 1b and e, lanes 7–8). Inhibition of polymerization by PolB was still observed upon varying the balance and decreasing the concentration of rNTPs (Fig. 1c and e, lane 6 compared with lanes 7–8). Taken together, these results show that the polymerization activity of PolD is much less affected by the balance and concentration of rNTPs compared with that of the p41/p46 complex. They also demonstrate the severe inhibitory effect of rNTPs on DNA primer extension activity by PolB.

When primer extension reactions were carried out with all eight nucleotides at ratios 1 and 2 in the presence of individual DNA Pols, the efficiency of primer extension was as high as with all four dNTPs (~82% extension) (Fig. 1e, lanes 4–5 compared with lanes 9–10). In this case, the profiles of polymerization for the two HiFi DNA Pols were almost comparable between the concentration ratios 1 and 2 of the four dNTPs only and all eight nucleotides (Fig. 1b–c, lanes 4–5 compared with lanes 9–10). By contrast, the p41/p46 complex suffered from the addition of rNTPs, as can be seen by the appearance of a prominent pause at +2 from the DNA primer (Fig. 1d, lanes 4–5 compared with lanes 9–10). In general, decreasing the concentrations of all eight nucleotides from ratio 1 to 2 did not significantly affect polymerization by the two HiFi DNA Pols, while leading to longer extension products by the p41/p46 complex (Fig. 1b–d, lanes 9–10). Only a 2-fold reduction of full-length product synthesis was observed with PolD, while expanding slightly with PolB (Fig. 1f, lanes 9–10). Overall, these results indicate that, in contrast with the two HiFi DNA Pols, the level of dNTPs/rNTPs affects DNA synthesis by the p41/p46 complex more strongly.

Incorporation of rNMPs into the primed-oligonucleotide DNA template

Because the three DNA Pols were able to add rNMPs (Fig. 1b–e, lanes 6–8) to the DNA primer and the length of extension products were maximized at ratio 2 for all three DNA Pols (Fig. 1b–e, lanes 9–10), we next evaluated the level of rNMP incorporation into a primed-oligonucleotide DNA template (Fig. 2). Extension products obtained from the 17-mer DNA primer annealed to the 87-mer template were treated with 0.25 M NaCl (control) or with 0.25 M NaOH to hydrolyze the DNA backbone at locations where rNMPs were present. The results show that the extension products generated by PolD were sensitive to NaOH treatment (Fig. 2a) in comparison with PolB (Fig. 2b) and the p41/46 complex (Fig. 2c). In this case, the 5′-labeled alkaline hydrolysis products resulted in the appearance of shorter fragments, which corresponded to ~+1, +2, +3 and + 4 rNMP additions from the DNA primers (Fig. 2a, intensity distribution traces). Although barely detectable, additional higher species accumulated at +10 with PolD. Therefore, these findings indicate that PolD is the only DNA Pol able to incorporate rNMPs into a short stretch of duplex DNA.

Incorporation of rNMPs into the primed-M13mp18 DNA template

To further evaluate the significance of PolD being the only one of the polymerases adept at rNMP incorporation into primed-oligonucleotide DNA template compared with PolB and the p41/p46 complex, extension reactions were carried out in the presence of a primer-template with a larger size,

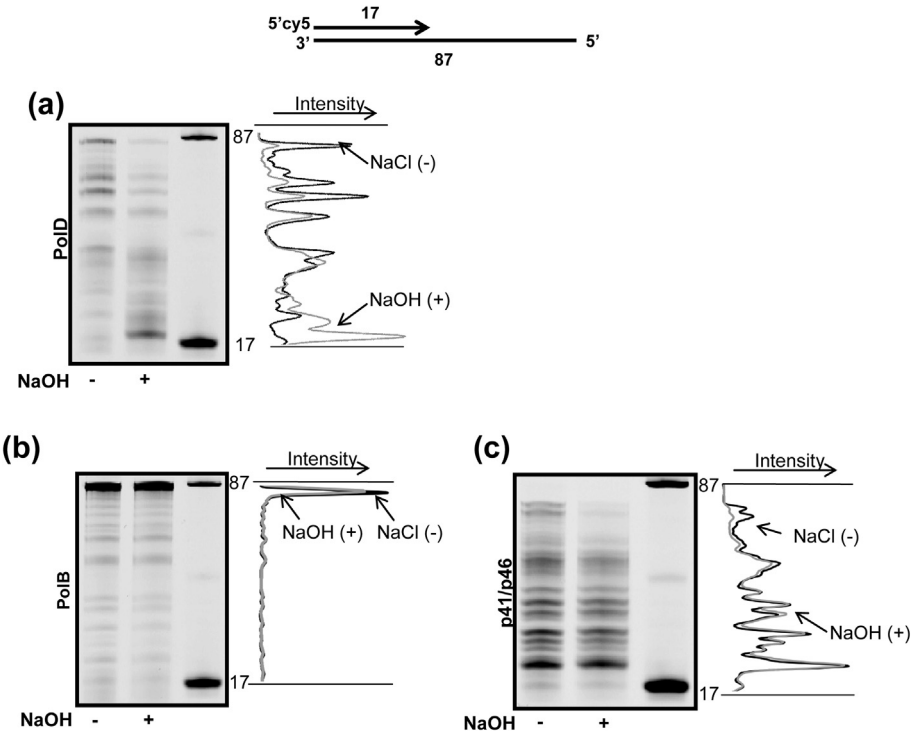

Fig. 2. Incorporation of rNMPs into duplex DNA (short DNA primer-template). The structure of the primer-template is represented at the top (for full sequences, see Table S1). (a–c) Extension reactions of the 5′-Cy5-labeled 17/87 primer-template using PolD (a), PolB (b) and the p41/p46 complex (c) with all four dNTPs at 5.6 μM dATP, 6.1 μM dGTP, 11.9 μM dTTP and 2 μM dCTP and all four rNTPs at 200 μM rATP, 128.4 μM rGTP, 112.4 μM rUTP and 58.4 μM rCTP (ratio 2). Samples were treated with either 0.25 M NaCl (denoted by NaOH−) or 0.25 M NaOH (denoted by NaOH+) are indicated under each gel. Reference oligodeoxynucleotides of 87 and 17 bases are indicated to the right of each panel. Densitometry traces of the NaCl (dark gray) and NaOH (pale gray) lines, plotted using Image Quant TL 8.1 software, are shown to the right of each gel image.

different topology and sequence (Fig. 3a). Since all three DNA Pols have been described to functionally interact with a variety of replisome components [34,35,49,50,52,53], the inclusion of accessory factors like PCNA may stimulate rNMP incorporation into the DNA.

Using primed-M13mp18 DNA template at the level of the nucleotides (ratio 1), matching those believed to exist in cells [2,3], PolD was highly efficient at inserting rNMPs into the DNA strands (Fig. 3b, lanes 19–20 compared with lanes 25–26; see the Cy5 panel). The extension products made by PolD in the presence of dNTPs were only unaffected by NaOH treatment (Fig. 3b, lane 25; see the Cy5 panel and Fig. S2b). By contrast, the elongated products obtained by adding rNTPs were converted by NaOH treatment to shorter fragments ranging from ~0.3 to 4 kb and, the estimated frequency of rNMP incorporation was approximately one rNMP every 1250 kb (Fig. 3b, lane 26; see the Cy5 panel). Illustrative densitometry traces of PolD incorporation are shown in Fig. 3b (PolD intensity distribution traces related to lanes 25–26) and the profile lines accounted for rNMP insertion throughout the newly synthesized DNA strands but also in the vicinity of the DNA primer. In addition, treatment of the polymerized strands with NaCl in the presence or absence of rNTPs did not affect the distribution of extension products (Fig. 3b, inset of the PolD intensity distribution traces related to lanes 19–20), which consisted of a mixture of ~+1 extended primers to full-length products (7249 nt). Overall, these results indicate that PolD is prone to embedding rNMPs into the newly synthesized strands and that rNMP incorporation only occurs at the same rNTP/dNTP ratios (ratios 1 and 2) (Figs. 3b and S1a). This finding is supported by the fact that PolD does not insert rNMPs at equimolar concentrations of all eight nucleotides (Fig. S1b, lanes 19–20 compared with lanes 25–26; see Cy5 panel).

PolB and the p41/p46 complex, by contrast, did not display rNMP incorporation into the DNA template (Fig. 3b, lanes 15–18 compared with lanes 21–24; see the Cy5 panel). PolB only polymerized dNTPs to yield a ladder of extension products from ~+1 to full length, of which the full-length fragments were the most prominent (Fig. 3b, lane 15; see the Cy5 panel). Addition of rNTPs resulted in the inhibition of primer

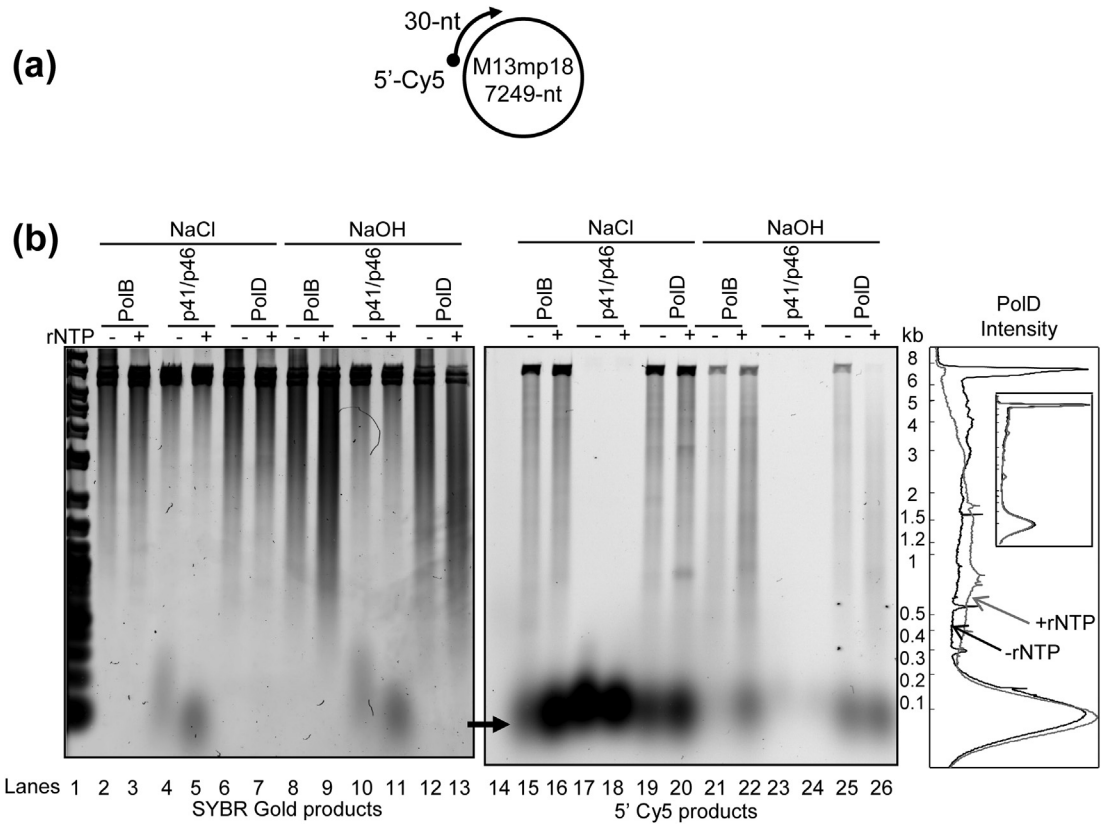

Fig. 3. Incorporation of rNMPs into the duplex DNA (M13mp18 DNA primer-template). (a) Structure of the primer-template mimic, consisting of a Cy5-labeled 30-mer primer annealed to the circular M13mp18 DNA template, 7249 nucleotides in length. (b) Extension of the primed-M13mp18 DNA template by PolB, the p41/p46 complex and PolD, with nucleotide substrates (ratio 1). Reactions contained the four dNTPs at 95 μM dATP, 103 μM dGTP, 200 μM dTTP and 33 μM dCTP with no additional rNTPs (denoted by −rNTP), or all eight nucleotides (denoted by +rNTP) at 95 μM dATP, 103 μM dGTP, 200 μM dTTP, 33 μM dCTP, 3359 μM rATP, 2157 μM rGTP, 1889 μM rUTP and 981 μM rCTP. Samples treated with either 0.25 M NaCl or 0.25 M NaOH are indicated at the top of each gel. The left and right gels refer to SYBR-Gold and Cy5-labeled products, respectively. The arrow on the left of the Cy5 panel indicates the starting DNA primers. Densitometric traces of the resulting PolD extension products after NaOH treatment (lanes 25–26) with rNTPs (pale gray line) or without rNTP (dark gray line) are shown with arrows to the right of the panels. The inset shows the densitometry traces of the resulting PolD extension products after NaCl treatment (lanes 19–20). Molecular weight markers (lanes 1 and 14) revealed by gel staining with SYBR Gold are labeled on the left of the densitometric representation.

extension, as shown by the increased level of primers (Fig. 3b, lane 16; see the Cy5 panel). These results are further supported by the densitometry traces, showing not only the higher abundance of primers but also the lower amounts of full-length products (Fig. S2b, PolB intensity distribution traces related to lanes 15–16). In addition, the inability of PolB to insert rNMPs into the DNA is in agreement with similar profiles obtained with NaCl (Fig. S2b, PolB intensity distribution traces related to lanes 15–16) and NaOH treatments of the polymerized strands (Fig. S2b, PolB intensity distribution traces related to lanes 21–22). Although barely detectable, the p41/p46 complex only polymerized dNMPs and addition of rNTPs resulted in the inhibition of primer extension (Fig. 3b, lanes 17–18 and 23–24; see the Cy5 panel). These results were further supported by the densitometry traces (Fig. S2b, p41/p46 intensity distribution traces related to lanes 17–18 and lanes 23–24). This low level of extension products was not due to differential loading amounts of replicated primed-M13mp18 DNA template compared with the SYBR Gold panel (Fig. 3b, lanes 4–5 and lanes 10–11). Moreover, addition of rNTPs was not only inhibitory to primer extension (Fig. 3b, lanes 17–18; see the Cy5 panel) but also to DNA priming activity by the p41/p46 complex (Fig. 3b, lanes 4–5; see the SYBR Gold panel). These findings show that neither PolB nor the p41/p46 complex can incorporate rNMPs into the DNA, a property that seems to be independent of the levels and balance of rNTPs and dNTPs (e.g., ratios 1 and 2, and equimolar concentrations) (Fig. S1a, lanes 15–18 and lanes 21–24; Fig. S1b, lanes 15–18 and lanes 21–24; see

the Cy5 panel). Taken together, these results demonstrate that PolD is the only DNA Pol capable of embedding rNMPs into newly polymerized DNA strands at physiological nucleotide concentrations and that PolB and the p41/p46 complex do not appreciably incorporate rNMPs into DNA. They also demonstrate that the frequency of rNMP insertion by PolD is governed by the level and balance of all eight nucleotides.

Levels of ribonucleotides in genomic DNA of wild-type and RNase HII null archaeal cells

Because rNMP incorporation into DNA occurs *in vitro* by PolD at physiological concentrations of all eight nucleotides, we verified whether rNMPs are incorporated into the genomes of exponentially growing archaeal cells. To address this possibility, the *in vivo* frequency of embedded rNMPs from two closely related euryarchaeal cells, *P. abyssi* and *Thermococcus barophilus*, was analyzed by alkali treatment followed by agarose gel electrophoresis. Alkali treatment causes strand cleavage at incorporated rNMPs in the DNA, resulting in increased electrophoretic mobility of genomic DNA. Given that alkali hydrolysis may also reveal local nicks, breaks and gaps, genomic DNA was treated with NaCl followed by agarose gel electrophoresis after formamide denaturation. This neutral formamide DNA denaturing method allows for the separation of single-stranded DNA without hydrolyzing rNMP phosphodiester bonds [54]. Treatment with NaOH led to an increased pattern of genomic DNA fragmentation from both wild-type archaeal cells relative to NaCl-treated DNA (Fig. 4a–b), whereas genomic DNA separated under neutral conditions did not demonstrate any significant fragmentation. These results indicate that the observed alkali-sensitive sites are consistent with the presence of rNMPs in genomic DNA of wild-type cells, but also suggest the existence of single-stranded interruptions (nicks or gaps). Moreover, treatment with alkali also led to a widespread fragmentation of RNase HII null genomic DNA from *T. barophilus*, observed by increased electrophoretic mobility (Fig. 4b). Significantly, the resulting pattern of fragmentation was different from that seen with wild-type genomic DNA, which on average leads to one rNMP per approximately 700 nt for the RNase HII

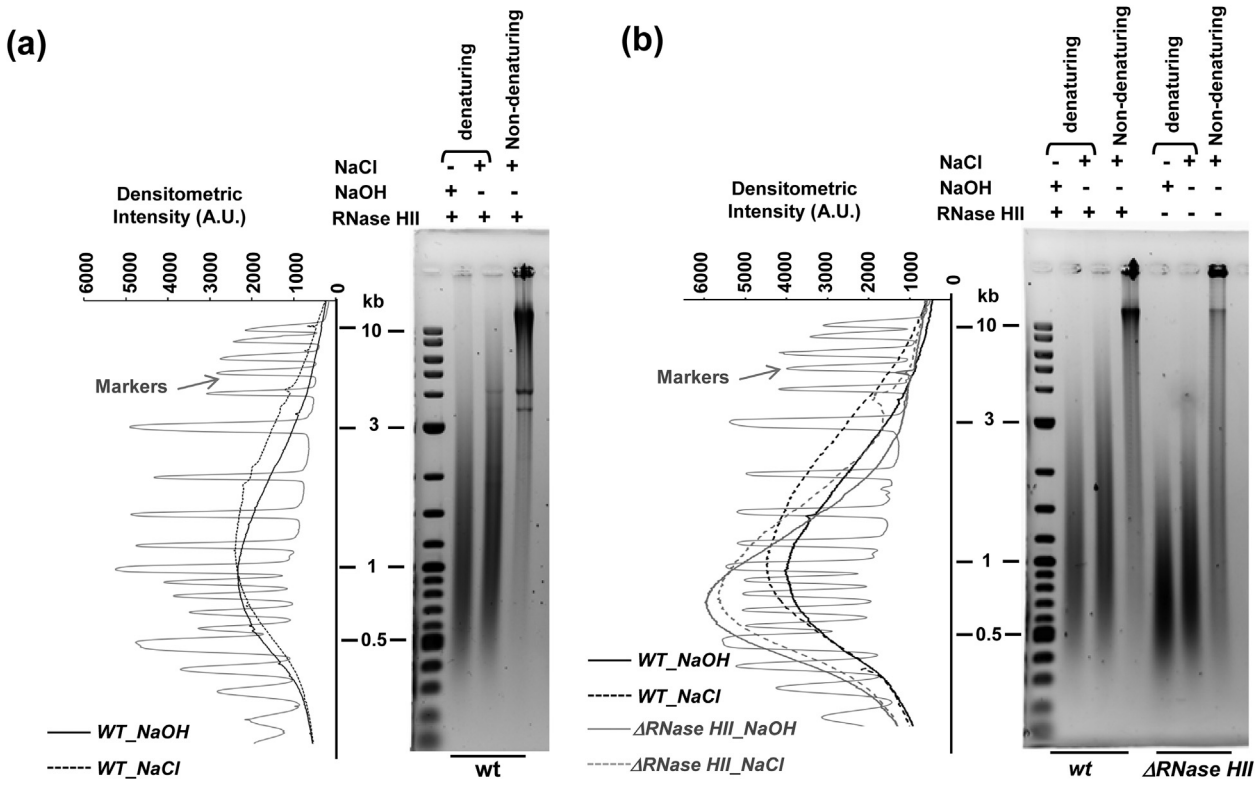

Fig. 4. Genomic detection of ribonucleotides in exponentially growing archaeal cells. (a) Alkali sensitivity of genomic DNA from wild-type *P. abyssi* cells. Separation by agarose gel electrophoresis under neutral conditions (non-denaturing) and after denaturation with formamide (denaturing). Densitometry analysis of the first two lanes is shown and size of the DNA markers indicated. (b) Alkali sensitivity of the genomic DNA from the wild-type and RNase HII null *T. barophilus* MP cells. Separation by agarose gel electrophoresis under neutral conditions (non-denaturing) and after denaturation with formamide (denaturing). Densitometry traces of selected lanes are shown, and size of the DNA markers is indicated.

mutant. Taken together, these data demonstrate that ribonucleotides accumulate at substantial levels in genomic DNA of archaeal cells, and that RNase HII is an enzyme involved in their repair.

Bypass of a single rNMP in a DNA Template

In the above experiments, we demonstrated that *P. abyssi* DNA PolD can efficiently incorporate rNTPs into DNA and that substantial levels of rNMPs are incorporated in the genome of *Archaea*. Because rNMPs persist in the template strand, we decided to analyze whether all three DNA Pols were able to tolerate ribonucleotide-containing templates. Therefore, we examined the ability of DNA Pols to bypass single embedded rUMP, rAMP, rGMP or rCMP located at the same position in the primer-template (i.e., 16 bases ahead of the 17/87 primer-template junction), corresponding to dTMP, dAMP, dGMP or dCMP in the control template (Fig. 5a). In general, DNA Pols were able to bypass each of the four different rNMPs (Fig. 5b–d), albeit at reduced efficiencies compared with the dNMP-containing templates (Fig. 5e). rUMP was the most inhibitory to primer-extension (<20% compared to ~87% with the dTMP control), followed by rCMP (<40% compared to ~87% with the dCMP control), then rAMP and rGMP (<75% compared to ~87% with the dAMP and dGMP controls, respectively). Examination of the patterns of replication products indicated

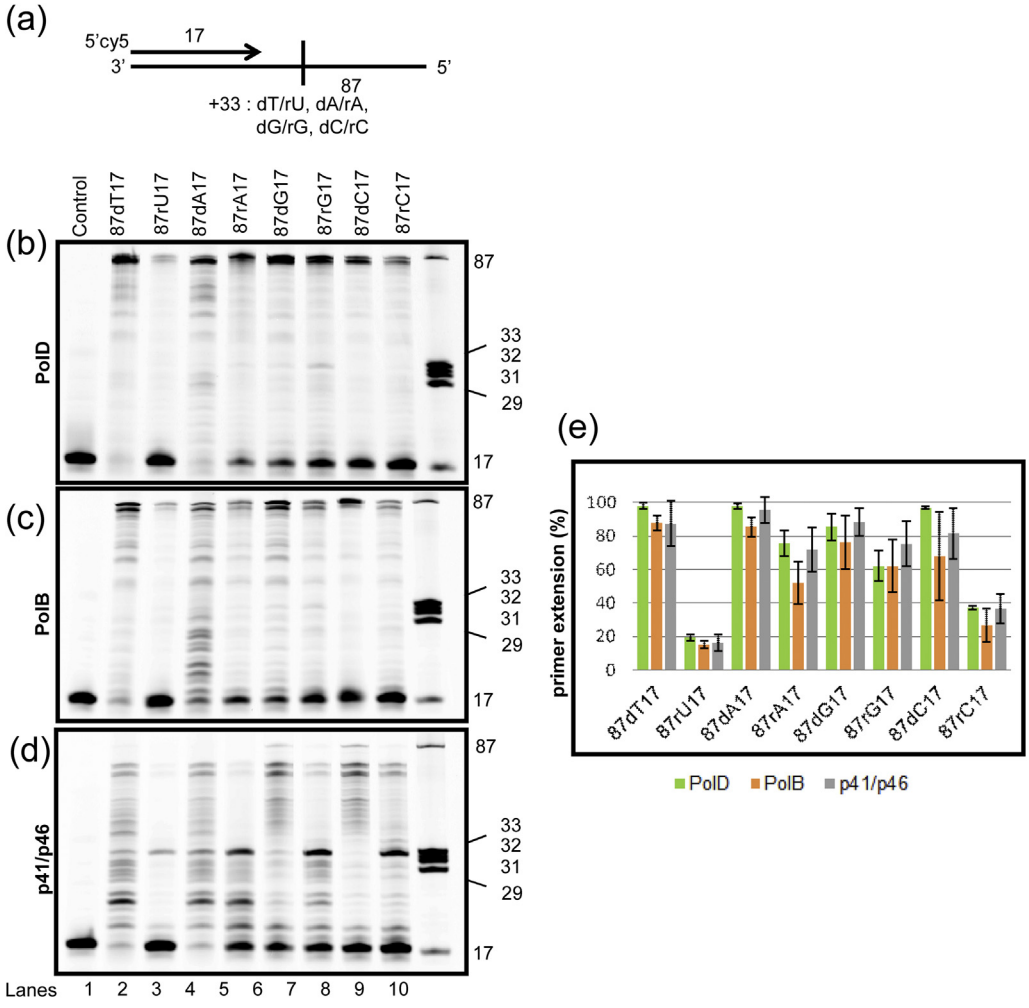

Fig. 5. Bypass of a single rNMP in a DNA Template. (a) Structure of the 5′-Cy5-labeled 17/87 primer-templates that locate either dNMP or rNMP 16 bases ahead of the primer-template junction. (for full sequences, see Table S1). (b–d) Extensions using PolD (b), PolB (c) and the p41/p46 complex (d) from *P. abyssi* during a 30-min reaction containing all four dNTPs. "Control" denotes the absence of dNTPs and $MgCl_2$. Reference oligodeoxynucleotides of 87, 33, 31, 29 and 17 bases are indicated on the right of each panel. Gel images of reaction products shown in panels b–d were quantified as described in Materials and Methods. (e) Bar graph summarizing extension products. Bars are the averages (±standard deviation) from at least three independent experiments.

that DNA Pols did not significantly stall during DNA synthesis (Fig. 5b–d). Compared to PolD and PolB, stalling was particularly strong for the p41/p46 complex with a noticeable arrest one nucleotide upstream of the rNMP (32-nt position) (quantification of the 32-nt products is given in Table S2), a difference that reflects abortive full-length DNA synthesis (Fig. 5d).

The gels shown in Fig. 5b–d indicate that rNMP-containing templates reduce DNA synthesis by DNA Pols. The inhibition could plausibly arise because RNA-dependent degradation of the template reduces the amount of available primer-templates. To address this possibility, 6-carboxyfluorescein-labeled templates containing each of the four rNMPs and annealed to the DNA primer were incubated with or without DNA Pols (Fig. S3). In no case did any of the DNA Pols cut rNMP-containing templates (Fig. S3a), excluding possible hydrolysis of the phosphodiester bond in an endonucleolytic manner. Moreover, strand cleavage caused by the presence of the 2'-OH of the ribose ring and accelerated at increased temperature [55] was never generated under our experimental conditions (Fig. S3, lane Control 1 = no enzyme added). Template degradation therefore cannot account for the inhibition of polymerization seen in the presence of rNMP.

Single-nucleotide incorporation opposite dNMP- or rNMP-containing templates by archaeal DNA Pols

To estimate the physiological relevance of rNTPs to the overall fidelity of DNA synthesis, we analyzed their incorporation opposite dNMP-containing templates. A series of 26-mer/34-mer primer-templates in which the first template base was varied (dCMP, dAMP, dTMP, or dGMP) were incubated with each of the four rNTPs and DNA Pols so that the DNA primer would be extended by only one ribonucleotide (rN). Figure 6a shows the results obtained with dCMP at the first template position. In this context, all three DNA Pols displayed significant dG incorporation (>90% incorporation), as expected (Fig. 6a, lane 5), although erroneous incorporation was also detected (Fig. 6a, lanes 3, 4 and 6). In the presence of a single rNTP, all three DNA Pols provided correct rG incorporation but the efficiency was less than dG. PolD showed a moderate decrease in incorporation levels with 23% and 95% for rG and dC, respectively (Fig. 6a, lanes 10 and 5). PolB and the p41/p46 complex suffered a marked decrease in incorporation levels with 16% and 90% for rG and dC, respectively, for PolB, compared with 3% and 98% for rG and dC, respectively, for the p41/p46 complex (Fig. 6a, lanes 10 and 5). In general, the ribonucleotide incorporation levels were reduced for all three DNA Pols and influenced by the dNMP template base (Figs. 6a and S4a, c, e; to compare lanes 2 and 7). In agreement with the results in Figs. 1–3, PolD was the most proficient for rN incorporation compared to PolB and the p41/p46 complex.

To further analyze the ribonucleotide incorporation capability of all three DNA Pols, single-nucleotide additions at the first template position were performed with rNMP-containing templates. In the control experiment, all three DNA Pols significantly incorporated dG opposite the rCMP template base (>60% incorporation) (Fig. 6b, lane 17) and showed minor misinsertion events (Fig. 6b, lanes 15, 16 and 18). Generally, all three DNA Pols achieved correct dN insertion opposite the canonical rNMP-containing template. PolB and PolD maintained comparable levels of dT or dC incorporation at the adenine or guanosine template base, independently of the identity of the sugar (Fig.S4a–b, lanes 4 and 16 and 5e–f, lanes 6 and 18). The level of dT incorporation remained stable opposite dAMP/rAMP-containing templates (~99/92% incorporation, respectively) for the p41/p46 complex (Fig. S4a–b, lanes 4 and 16), while a minor decrease in dC incorporation efficiency (~1.5-fold reduction in incorporation) due to the sugar variation was observed (Fig. S4e–f, lanes 6 and 18). When the experiments were repeated with dCMP/rCMP- or dTMP/rUMP-containing templates, a reduction of dG (Fig. 6a–b, lanes 5 and 17) or dA (Fig. S4c–d, lanes 3 and 15) incorporation efficiency was noticeable for all three DNA Pols, but this effect was more pronounced for the p41/p46 complex. Overall, these results are consistent with the bypass properties of DNA Pols observed in Fig. 5, demonstrating that the gradual reduction of dN incorporation is governed by both the identity of the sugar and the template base. The priority order for dN insertion opposite the rNMP-containing template is thus rG = rA > rC > rU.

When the reactions were carried out with each of the four rNTPs and the rNMP-containing templates, neither PolB nor the p41/p46 complex was able to extend the DNA primer (Figs. 6b, S4b, d and f, lanes 20–23). Also, the exonuclease activity of PolB was particularly enhanced with rAMP- and rUMP-containing templates (Fig. S4b and d, lanes 15–23). Conversely, PolD correctly base-paired a single ribonucleotide opposite rNMP-containing templates, but this insertion only occurred at the cytosine and guanine template bases (Fig. 6, lane 22 and Fig. S4f, lane 23). In this case, the incorporation efficiency was higher at rCMP compared with rGMP-containing templates (75% and 47% incorporation, respectively). Interestingly, when all four rNTPs were simultaneously added, PolD could generate similar amounts of extension products opposite the cytosine and guanine template bases (75% and 34% incorporation, respectively), while showing different extension behaviour (Figs. 6b and S4f, lane 19). The enzyme was able to insert and extend the DNA primer from multiple consecutive ribonucleotides (up to six rN additions), and the distribution of longer products was more

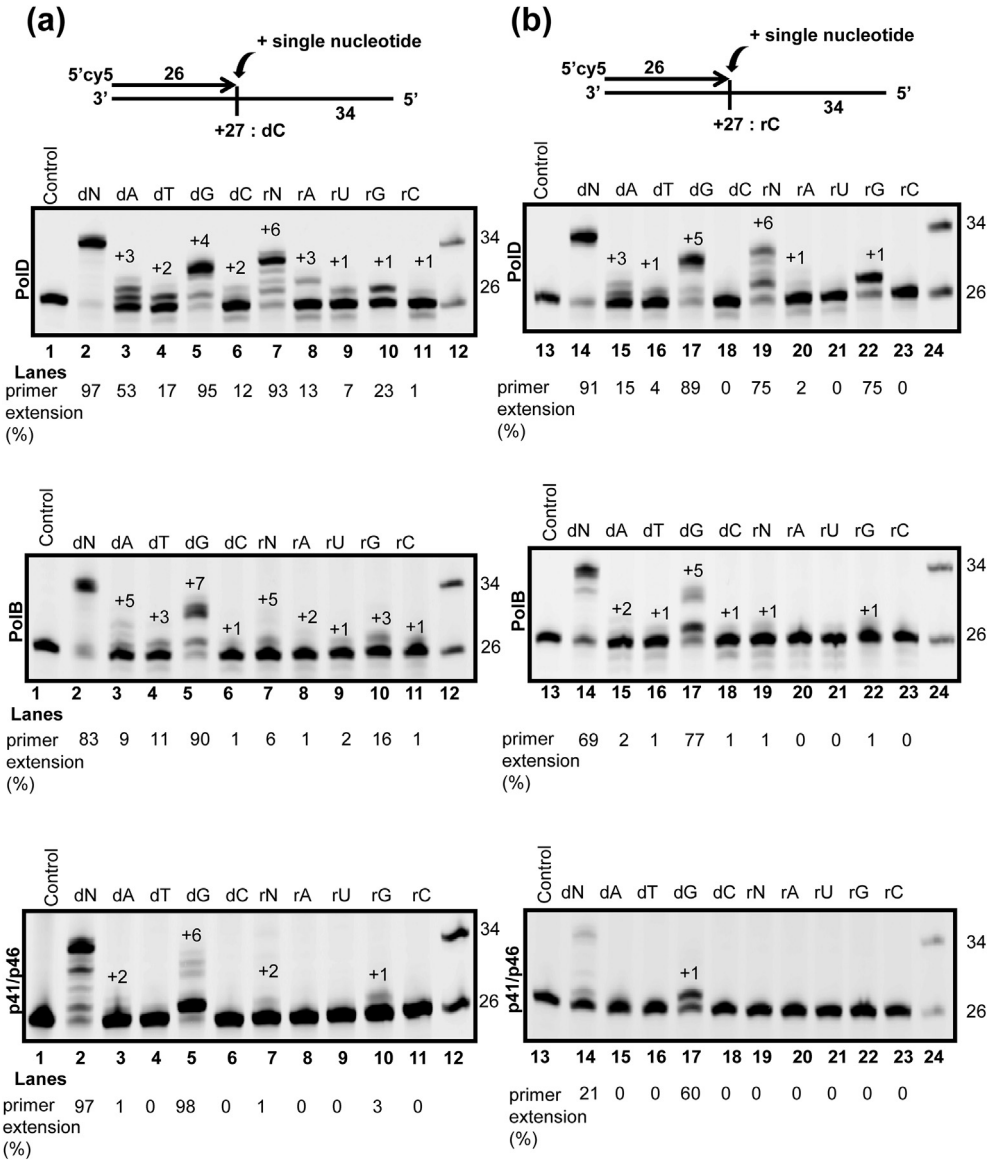

Fig. 6. Single-nucleotide incorporation opposite dCMP- or rCMP-containing template. DNA primer extension reaction of the 5′-Cy5-labeled 26/34 primer-templates that locate dCMP or rCMP one base ahead of the primer-template junction. The structure of the primer-template is represented at the top of each panel (for full sequences, see Table S1). (a) Base incorporation opposite template strand dCMP by PolD, PolB and the p41/p46 complex. (b) Base incorporation opposite template strand rCMP by PolD, PolB and the p41/p46 complex. Each reaction had a running time of 30 min. "Control" = no enzyme added (lanes 1 and 13); dN = all four dNTPs added; dA, dT, dG and dC = only dATP or dTTP or dGTP or dCTP added, respectively; rN = all four rNTPs added; rA, rU, rG and rC = only rATP or rUTP or rGTP or rCTP added, respectively; +1, +2, +3, +4, +5 and + 6 represent final products. The extension (%) for selected lanes is shown under the gels. Reference oligodeoxynucleotides of 34 and 26 bases are indicated on the right of each panel (lanes 12 and 24).

pronounced in the presence of rCMP-containing templates (Figs. 6b and S4f, lane 19). Taken together, these results clearly demonstrate that PolD has the highest propensity to faithfully extend a DNA primer from one to multiple consecutive rN on dNMP-containing templates. Although unexpected, PolD also displays rN incorporation on rNMP-containing templates, occurring with high specificity in an error-free manner.

Discussion

Nucleotide pools in archaeal cells. What similarities exist across the three domains of life?

In the present study, we determined for the first time the nucleotide pools in an anaerobic and hyperthermophilic euryarchaeal strain. The results

indicate that the relative size of each dNTP pool varied, with dTTP being the largest and dCTP being the smallest in exponentially growing *P. abyssi* cells. Apart from a few exceptions, the elevated level of dTTP seems to reflect that obtained from other organisms across the three domains of life [2–5]. Interestingly, it appears that dTTP > dGTP are the most abundant dNTPs in archaeal cells [5], thus contrasting with total cellular or nuclear dNTP pools, where dGTP is consistently observed to be the least abundant DNA precursor [2,3,4,56]. However, the high level of dGTP in *Archaea* resembles that of mitochondria, with dGTP predominating in many tissues [57]. Compared with dNTPs, the relative size of each rNTP pool also varied, with rATP the most abundant and rCTP the lowest. These results confirm the ubiquitous nature of the rATP molecule in all organisms [2–5], involved not only in energy metabolism and signaling but also in RNA synthesis. The current report also demonstrates that *P. abyssi* proliferating cells have an excess of rNTPs over dNTPs, ranging from 9 to 35 for rUTP/dTTP and rATP/dATP, respectively. Because rATP is the most abundant rNTP, the rATP/dATP ratio is the highest in all organisms. However, the rNTP/dNTP pools are not balanced similarly [2–5]. For instance, we observed that intracellular rNTP/dNTP ratios resemble each other in the crenarchaeal *Sulfolobus solfataricus* strain, apart from the ratio of rATP/dATP [5]. By contrast, all rNTP/dNTP ratios are well balanced in exponentially growing *P. abyssi* cells, thus reflecting another distinction between the major subdivisions Crenarchaea and Euryarchaea within the archaeal domain [58].

Are ribonucleotides incorporated into DNA by the three DNA-dependent polymerizing enzymes in *P. abyssi*?

All studies to date have revealed evidence that cellular DNA Pols incorporate rNMPs during DNA synthesis, likely due to the high relative cellular pools of rNTP compared with dNTP as recently published and reviewed [2,12,14,16,59–61]. Based on the cellular ratios of rNTPs/dNTPs in *P. abyssi*, we predicted that the three DNA dependent polymerizing enzymes (PolD, PolB and the p41/p46 complex) [31,35] might display rNMP incorporation. Our results indicate that rNMPs are mainly incorporated into the DNA by the family-D DNA Pol at the physiological level of nucleotides. The estimated frequency of rNMP incorporation determined by alkaline treatment is approximately one rNMP every 1250 kb (Fig. 3b, lane 26; see the Cy5 panel). Thus, ~2800 rNMPs could theoretically be introduced into the genome of *P. abyssi* during each round of DNA replication, assuming that PolD simultaneously synthesizes the leading and lagging strands at the fork *in vivo.* However, this number could be reduced to ~1400 rNMPs per round of lagging strand replication by PolD if PolB and PolD are responsible for the bulk of leading and lagging strand DNA synthesis, respectively. Because PolD is the most adept at rNMP incorporation, finding rNMPs in a particular strand (either leading or lagging) would suggest that PolD is responsible for the synthesis of this particular strand. Such hypotheses now require further investigation to clarify the role of the DNA Pol(s) in genome replication in Euryarchaea.

Nevertheless, the current report demonstrates that rNMP incorporation is evolutionarily conserved among the three domains of life. Our *in vitro* and *in vivo* measurements are clearly consistent with rNMP accumulation in the genome of archaeal cells as a consequence of incorporation by DNA Pols. However, the density of rNMPs alone cannot account for rNMP incorporation by DNA Pol, particularly by PolD. Indeed, the frequency of embedded rNMPs (one per approximately 700 nt) determined by alkaline treatment in genomic DNA from RNase HII null archaeal cells (Fig. 4b) does not correlate with the average rNMP incorporation frequency of PolD (one per approximately 1250 nt) (Fig. 3b, lane 26; Cy5 panel). This suggests that embedded rNMPs in archaeal genomes could potentially result from other sources. Interestingly, we also observed that *Archaea* evolved a significant steady-state level of rNMPs, as deduced from the sensitivity of their genomic DNA to alkaline hydrolysis in two wild-type euryarchaeal cells. This is of particular importance since their genome exhibits a substantially high gene-coding percentage (~90%). Hence, this suggests that rNMPs are regularly incorporated into the genome of *Archaea*, potentially exceeding the rNMP incorporation frequency in the genomes of *Bacteria* [17] and eukaryotes [2,62]. Further work is now required to determine the distribution, frequency, identity and density of ribonucleotides in the archaeal genome.

Our results also demonstrate that PolD correctly base-paired a single rNMP opposite the template base, a feature that can be influenced by the sequence context but also by the nature of the nucleotide to be incorporated. These data suggest that PolD discriminates differently against rNTPs, thus awaiting the determination of its selectivity for the four nucleotides. In addition, we discovered that the frequency of rNMP incorporation by PolD could be influenced not only by the level but also by the balance of the rNTP and dNTP pools. For instance, we observed that normalizing the rNTP and dNTP levels to equimolar concentrations shifted the polymerase activity exclusively to DNA synthesis. In the future, it would be of interest to determine the threshold of the rNTP/dNTP pool balance which can dictate rNMP incorporation by PolD. Despite a recent report on the PolD complex structure, supporting rNMP incorporation because of its strong structural homology

with the active site of RNA polymerases [63], the molecular mechanism involved in sugar discrimination in the presence of magnesium remains unsolved and awaits the structural resolution of the ternary complex (PolD/DNA/nucleotide).

As mentioned above, neither PolB nor the p41/p46 complex was able to incorporate rNMPs into DNA at physiological nucleotide levels. Characterized here as template-dependent DNA Pols, they strongly discriminate against NTPs, a feature that correlates with the identification of a presumed steric gate in the vicinity of their active site [64,65]. However, these results do not preclude rNMP insertion by these two enzymes *in vivo*. Indeed, here we showed that both enzymes could incorporate rNMPs under particular reaction conditions *in vitro* (e.g., single-nucleotide incorporation or primer extension with only rNTPs as nucleotide substrates). Moreover, recent findings carried out with the closely related *Thermococcus kodakaraensis* demonstrated that not only PolD but also PolB were capable of inserting rNMPs during DNA synthesis [14]. The cellular concentration of rNTPs and dNTPs provided to these archaeal DNA Pols were those of the wild-type eukaryotic *S. cerevisiae* and thus relatively higher than the physiological ones, which might explain why PolB from *T. kodakaraensis* was rendered permissive to rNMP incorporation. These observations suggest that sugar discrimination during nucleotide substrate selection is not absolute, and that both PolB and the p41/p46 complex might display relaxed specificity under certain growth conditions (changes in the balance and ratio of dNTPs/rNTPs, metal ion concentrations, *etc.*).

We also observed that the presence of rNTPs stimulated DNA synthesis of longer products by PolB when all eight nucleotides are added at low levels (Fig. S1a). One possible explanation would be that rNTPs function as regulatory molecules, shifting the exo/pol balance of PolB into a more processive elongation mode at minimal nucleotide pool sizes *in vivo*. When present at higher levels, rNTPs also affected DNA synthesis ability by PolB and the p41/p46 complex (Fig. 3b). In this case, decreased amounts of utilized primers and reduced DNA priming activity by the p41/p46 complex were observed, again demonstrating a regulatory role by rNTPs on DNA synthesis. Hence, the molecular mechanism underlying the regulatory specificities of rNTPs on DNA Pol activity requires deeper investigation.

What are the effects of rNMP persistence in genomic DNA on polymerization activities by the three DNA Pols?

Our data and those from Heider *et al.* [14] indicate that the archaeal genome naturally contains embedded ribonucleotides and a loss of type 2 RNase H results in increased rNMP load. Our extensive exploration of bypass capacity of a single rNMP demonstrates that all three enzymes can replicate across an embedded rNMP in DNA. However, a gradual reduction of dN incorporation opposite the rNMP-containing template appears to be governed by both the identity of the sugar and the template base, in which template rUMP is the highest inhibitory. Compared with PolD and PolB, the p41/p46 complex is the most sensitive to rNMP-containing template, showing pausing one base ahead of rNMP residues. Possibly, pausing near the rNMP sites of the DNA template might serve as a relevant signal for coordinating DNA transactions (e.g., DNA repair, DNA Pols switching, *etc.*). It would thus be interesting to analyze whether embedded rNMPs in DNA can affect replication fork progression in *Archaea.* Although unexpected, PolD correctly base-paired a single ribonucleotide opposite rNMP-containing templates, but this insertion only occurred at the cytosine and guanine template bases. This is the first time that a DNA-dependent-DNA Pol has been shown to be able to insert a single ribonucleotide opposite embedded rNMP in the DNA template with such specific ribosignatures. Moreover, in addition to inserting a single ribonucleotide opposite rNMP-containing templates, PolD was able to polymerize multiple consecutive ribonucleotides (up to six rN additions to the primer). This result suggests a potential mechanism for the generation of dsRNA segments in genomic DNA in *Archaea* by the family-D DNA Pol.

What could be the physiological roles of rNMP incorporation into the DNA of *Archaea*?

According to our *in vivo* alkali detection and genetic evidence, archaeal cells accumulating rNMPs into the genome of the wild-type and type 2 RNase H mutant do not show obvious growth variations and tolerate them well [14,15]. Moreover, the ribonucleotide bypass shown in this study was not mutagenic, suggesting that *Archaea* evolved to replicate such nonstandard nucleotides in DNA. Although the abundance, identification and distribution of rNMPs across the archaeal genomes are not yet available, our results sustained prominent rNMP incorporation by PolD, suggesting that rNMPs "left over" after repairs may have particular signaling functions. As such, archaeal cells could use rNMP as a marker for the recognition of newly synthesized strands during post-replicative DNA repair pathways (e.g., MMR or Top1-RER) [22,23]. Despite the recent identification of MMR in *Archaea* [66], it remains to be determined whether these two repair systems are operational. In addition, it cannot be excluded that additional rNMP-induced DNA damage responses could be at work in archaeal cells (e.g., double-strand breaks (DSBs) repair mechanisms, RER, *etc.*). Finally, because of the unique signatures of rNMP incorporation opposite a single rNMP embedded into DNA

by PolD, spontaneous DNA hydrolysis may occur nonrandomly in the genome. Hence, endogenous hotspots of DSBs could be relevant to archaeal mating, or/and to the frequent chromosomal DNA exchange and horizontal gene transfer in *Archaea* [67,68]. Whether rNMP hotspots in the generation of DSBs participate in DNA exchange remains to be established.

Materials and Methods

Culture conditions

P. abyssi GE5, *T. barophilus* MP wild-type and *T. barophilus* MP RNase HII null cells were grown in a gas-lift bioreactor under anaerobic conditions at 90 °C and 85 °C, respectively, as previously described [15,69,70]. Exponentially growing cells were collected, centrifuged and stored at −80 °C under strict anaerobia.

Determination of dNTP and rNTP pools

At densities from 2.4×10^8 to 8.75×10^9 cells/mL, 1.26×10^{12} cells were harvested by centrifugation at 15,000*g* for 60 min at 4 °C. Cell pellets were immersed in 700 µL of ice-cold TCA/$MgCL_2$ solution (12% w/*v* trichloroacetic acid and 15 mM $MgCl_2$) and flash frozen in liquid nitrogen. The following steps were carried out, as recently published [71]. dNTP and rNTP levels (pmol/cells) in Table 1 were used to define two cellular concentrations (ratios 1 and 2). The reference for calculating the balance with the seven remaining nucleotides in ratio 1 was 200 µM dTTP, resembling levels believed to normally occur in *Bacteria* and *Eukarya* [2,3]. The rNTP reference for calculating the balance with the seven remaining nucleotides in ratio 2 was 200 µM rATP. The basal references of these two ratios were used throughout this study because they correspond to previous working nucleotide concentrations (200 µM of either dNTPs or rNTPs) supplied to *P. abyssi* DNA Pols in extension assays [31,35].

Detection of ribonucleotides in genomic DNA

Cell pellets (~0.5 µg) were suspended in 1.6 mL TE [10 mM Tris–HCl (pH 8), 1 mM Na_2EDTA]. To ensure cell lysis, 100 µL proteinase K (20 mg/mL), 200 µL Sarkosyl (10%) and 200 µL SDS (10%) were added followed by subsequent incubation at 37 °C for 1.5 h. Isolation of total DNAs was accomplished by adding an equal volume of buffered (pH 8.0) Phenol/chloroform/isoamylalcohol (25:24:1). The DNA solution was gently mixed and the aqueous phases were collected by centrifugation at 10,000*g* for 10 min at 4 °C (done twice). Then 10 µL of RNase A (10 mg/mL) was added and the mix was incubated at 37 °C for 1 h. DNAs were purified with an equal volume of phenol/chloroform/isoamylalcohol and centrifuged. The upper phase was extracted with an equal volume of pure chloroform and centrifuged. DNA precipitation was obtained by mixing the final aqueous phase with a 0.7 volume of 100% isopropanol followed by incubation for 1 h at room temperature. After a 30-min centrifugation at 15,000*g* at 4 °C, the DNA pellets were washed once with 0.5 mL of 70% ice-cold ethanol. Finally, the DNA pellets were air-dried for 45 min before suspension in TE [10 mM Tris–HCl, 1 mM Na_2EDTA (pH 8)].

For detection of ribonucleotides, genomic DNAs isolated from wild-type and RNase HII null archaeal cells were heated for 2 h at 55 °C with either 0.3 M NaOH or 0.3 M NaCl. Samples were ethanol precipitated and separated on 1× TBE agarose gel (1%) electrophoresis under neutral conditions [5% glycerol, 1.7 mM Tris–HCl (pH 8), 0.17 mM Na_2EDTA] or after denaturation with 90% formamide and 20 mM EDTA. Gels were then stained with ethidium bromide. Densitometry traces were obtained with Quantity One software 4.6.6 (Bio-Rad) and plotted as follows: each lane profile was extracted from the gel image and the background subtracted. The quantification of DNA fragmentation pattern was calculated from densitometry traces as follows: densitometry intensity distribution was divided by the fragment length distribution to quantify the proportion of molecules of a particular fragment size.

Enzymes

All DNA Pols used in this study were cloned, overexpressed and purified as previously described in the following articles: PolB [51], PolD [42] and the p41/p46 complex [72]. PCNA was produced and purified as described in Ref. [73].

Nucleic acids

Premium quality-unlabeled dNTPs and rNTPs were purchased from Jena Bioscience. sscM13mp18 (single-stranded circular M13mp18 DNA) were purchased from New England BioLabs (NEB). Oligonucleotides used in primer extension assays were RP-HPLC purified and purchased from Eurogentec (Seraing, Belgium) with the exception of the 87-mer oligonucleotides, which were purified by PAGE. Their sequences are listed in Table S1. Annealing of two complementary oligonucleotides was performed at equimolar concentrations in 10 mM Tris–HCl (pH 8) and 50 mM NaCl. The mixture was heated to 95 °C for 5 min and slowly cooled to room temperature. Annealing of sscM13mp18 to the complementary primers was carried out at 1:3 molar ratio in 300 mM NaCl, 20 mM Tris–HCl (pH 8) and 1 mM EDTA, by

heating to 75 °C for 15 min followed by cooling to room temperature.

Primer extension reactions

Extension of the fluorescent-labeled primer annealed to the oligodeoxynucleotide DNA template (50 nM) was carried out in reaction mixtures (20 μL) of 50 mM Tris–HCl (pH 8), 1 mM DTT, 0.2 mM EDTA, 50 mM NaCl and 5 mM $MgCl_2$, with only the four dNTPs (200 μM or at the indicated physiological ratio), only the four rNTPs (at 200 μM or the indicated physiological ratio), or all eight nucleotides at the indicated cellular concentrations. The polymerases used were 100 nM of PolD, 100 nM of the p41/p46 complex and 6.25 nM of PolB, and the incubations were made at 55 °C for 30 min. For detection of rNMP incorporation into DNA, reactions were quenched on ice by adding an equal volume of 20 mM EDTA. Half of the reaction mixtures (20 μL) were then incubated at 55 °C for 2 h with either 0.25 M NaCl or 0.25 M NaOH. The mixtures were kept on ice and stopped by adding one volume of 98% deionized formamide and 20 mM EDTA. For single-nucleotide incorporation, a single nucleotide was added at 200 μM (final concentration). Reactions with PolD, PolB and the p41/p46 complex were stopped on ice by adding 20 μL of stop buffer [98% deionized formamide, 10 mM NaOH, 10 mM EDTA (pH 8), 1 μM of "oligonucleotide competitor" (the exact complement of the template strand under study)] and samples were heated to 95 °C for 5 min, before being loaded onto 18% denaturing polyacrylamide gels. Labeled fragments were detected with Typhoon FLA 9500 (GE Healthcare) and quantified with Image Quant TL 8.1 (GE Healthcare). The quantification methods were as follows: extension of the primers (%), intensity of primers as a percentage of total lane intensity; full-length 87-nt (%), intensity of 87-nt bands as a percentage of total lane intensity; stall (%), intensity of identified stall band as a percentage of total lane intensity. Densitometry traces were obtained using Image Quant TL 8.1 software (GE Healthcare) and plotted by extracting each lane profile from the gel image, subtracting the background, and further normalizing by the total lane intensity.

Extension reactions of the fluorescent-labeled 30-mer primer annealed to the sscM13mp18 template (7 nM) were performed in 25 μL of 50 mM Tris–HCl (pH 8), 1 mM DTT, 0.2 mM EDTA, 50 mM NaCl, 5 mM $MgCl_2$, and either just the four dNTPs (200 μM or at the indicated cellular concentrations) or all eight nucleotides (at 200 μM or the indicated cellular concentrations). For the polymerases, 1 μM of PolD, 1 μM of the p41/p46 complex, 100 nM of PolB and PCNA (300 nM, 300 nM and 30 nM in the DNA Pols, respectively). Primer-extension reactions were carried out at 55 °C for 180 min and quenched on ice by addition of EDTA (10 mM final concentration). Half of each reaction mixture was incubated at 55 °C for 2 h with either 0.25 M NaCl or 0.25 M NaOH. The mixtures were kept on ice and stopped by adding one volume of 90% deionized formamide and 20 mM EDTA. Samples were heated to 95 °C for 5 min before being loaded onto 1% (w/v) alkaline agarose gel. DNA ladders (2-Log DNA ladders, NEB) were loaded in 45% deionized formamide and 10 mM EDTA and run into the same gel at 4 °C for 15 h at 30 V. After electrophoresis, gels were stained with SYBR Gold (Invitrogen). Gels were first scanned with a Mode Imager Typhoon 9500 (GE Healthcare) for Cy5 in order to visualize the Cy5-labeled products, and then scanned for SYBR Gold for detecting all fragments. Densitometry traces were obtained using Image Quant TL 8.1 software (GE Healthcare) and plotted as follows: each lane profile was extracted from the gel image, had its background subtracted, and was further normalized by the total lane intensity.

Acknowledgments

Mélanie Lemor thanks the French Institute for the Exploitation of the Sea (Ifremer) and the Regional Council of Brittany for funding. The dNTP/rNTP measurements were performed in the laboratory of Dr. Chabes, Umeå University. This work was supported by the French National Research Agency (ANR-10-JCJC-1501-01 to G.H.). Funding for the open access charge was provided by the French National Research Agency (ANR).

Declaration of Interest: None.

Appendix A. Supplementary data

Supplementary data to this article can be found online at https://doi.org/10.1016/j.jmb.2018.10.004.

Received 2 July 2018;
Received in revised form 9 September 2018;
Accepted 12 October 2018
Available online 31 October 2018

Keywords:
Archaea;
DNA replication and repair;
DNA polymerase;
Nucleotide pool;
Translesion synthesis

Abbreviations used:
rNMPs, incorporated ribonucleotides; dNTPs, deoxyribonucleotides; rNTPs, ribonucleotides; DNA Pol, DNA polymerase; HiFi DNA Pol, high-fidelity DNA polymerase; RNase H, ribonuclease H; Top, topoisomerase.

References

[1] B.A. Kunz, S.E. Kohalmi, T.A. Kunkel, C.K. Mathews, E.M. McIntosh, J.A. Reidy, International Commission for Protection Against Environmental Mutagens and Carcinogens. Deoxyribonucleoside triphosphate levels: a critical factor in the maintenance of genetic stability, Mutat. Res. 318 (1994) 1–64.

[2] S.A. Nick McElhinny, B.E. Watts, D. Kumar, D.L. Watt, E.B. Lundstrom, P.M. Burgers, E. Johansson, A. Chabes, T.A. Kunkel, Abundant ribonucleotide incorporation into DNA by yeast replicative polymerases, Proc. Natl. Acad. Sci. U. S. A. 107 (2010) 4949–4954.

[3] M.H. Buckstein, J. He, H. Rubin, Characterization of nucleotide pools as a function of physiological state in *Escherichia coli*, J. Bacteriol. 190 (2008) 718–726.

[4] T.W. Traut, Physiological concentrations of purines and pyrimidines, Mol. Cell. Biochem. 140 (1994) 1–22.

[5] L.P. Liew, Z.Y. Lim, M. Cohen, Z. Kong, L. Marjavaara, A. Chabes, S.D. Bell, Hydroxyurea-mediated cytotoxicity without inhibition of ribonucleotide reductase, Cell Rep. 17 (2016) 1657–1670.

[6] T.A. Kunkel, Evolving views of DNA replication (in)fidelity, Cold Spring Harb. Symp. Quant. Biol. 74 (2009) 91–101.

[7] R.M. Schaaper, Base selection, proofreading, and mismatch repair during DNA replication in *Escherichia coli*, J. Biol. Chem. 268 (1993) 23762–23765.

[8] J.A. Brown, Z. Suo, Unlocking the sugar "steric gate" of DNA polymerases, Biochemistry 50 (2011) 1135–1142.

[9] A.R. Clausen, S. Zhang, P.M. Burgers, M.Y. Lee, T.A. Kunkel, Ribonucleotide incorporation, proofreading and bypass by human DNA polymerase delta, DNA Repair (Amst) 12 (2013) 121–127.

[10] J.S. Williams, A.R. Clausen, S.A. Nick McElhinny, B.E. Watts, E. Johansson, T.A. Kunkel, Proofreading of ribonucleotides inserted into DNA by yeast DNA polymerase epsilon, DNA Repair (Amst) 11 (2012) 649–656.

[11] S.A. Nick McElhinny, D. Kumar, A.B. Clark, D.L. Watt, B.E. Watts, E.B. Lundstrom, E. Johansson, A. Chabes, T.A. Kunkel, Genome instability due to ribonucleotide incorporation into DNA, Nat. Chem. Biol. 6 (2010) 774–781.

[12] N.Y. Yao, J.W. Schroeder, O. Yurieva, L.A. Simmons, M.E. O'Donnell, Cost of rNTP/dNTP pool imbalance at the replication fork, Proc. Natl. Acad. Sci. U. S. A. 110 (2013) 12942–12947.

[13] J.A. Rumbaugh, R.S. Murante, S. Shi, R.A. Bambara, Creation and removal of embedded ribonucleotides in chromosomal DNA during mammalian Okazaki fragment processing, J. Biol. Chem. 272 (1997) 22591–22599.

[14] M.R. Heider, B.W. Burkhart, T.J. Santangelo, A.F. Gardner, Defining the RNaseH2 enzyme-initiated ribonucleotide excision repair pathway in *Archaea*, J. Biol. Chem. 292 (2017) 8835–8845.

[15] T. Birien, A. Thiel, G. Henneke, D. Flament, Y. Moalic, M. Jebbar, Development of an effective 6-methylpurine counter-selection marker for genetic manipulation in *Thermococcus barophilus*, Genes (Basel) 9 (2018).

[16] J.W. Schroeder, J.R. Randall, W.G. Hirst, M.E. O'Donnell, L.A. Simmons, Mutagenic cost of ribonucleotides in bacterial DNA, Proc. Natl. Acad. Sci. U. S. A. 114 (2017) 11733–11738.

[17] E.A. Kouzminova, F.F. Kadyrov, A. Kuzminov, RNase HII saves rnhA mutant *Escherichia coli* from R-loop-associated chromosomal fragmentation, J. Mol. Biol. 429 (2017) 2873–2894.

[18] K.D. Koh, H.C. Chiu, E. Riedo, F. Storici, Measuring the elasticity of ribonucleotide(s)-containing DNA molecules using AFM, Methods Mol. Biol. 1297 (2015) 43–57.

[19] J.L. Sparks, H. Chon, S.M. Cerritelli, T.A. Kunkel, E. Johansson, R.J. Crouch, P.M. Burgers, RNase H2-initiated ribonucleotide excision repair, Mol. Cell 47 (2012) 980–986.

[20] A. Vaisman, J.P. McDonald, S. Noll, D. Huston, G. Loeb, M.F. Goodman, R. Woodgate, Investigating the mechanisms of ribonucleotide excision repair in *Escherichia coli*, Mutat. Res. 761 (2014) 21–33.

[21] S.N. Huang, J.S. Williams, M.E. Arana, T.A. Kunkel, Y. Pommier, Topoisomerase I-mediated cleavage at unrepaired ribonucleotides generates DNA double-strand breaks, EMBO J. 36 (2017) 361–373.

[22] J.S. Williams, D.J. Smith, L. Marjavaara, S.A. Lujan, A. Chabes, T.A. Kunkel, Topoisomerase 1-mediated removal of ribonucleotides from nascent leading-strand DNA, Mol. Cell 49 (2013) 1010–1015.

[23] Y. Shen, K.D. Koh, B. Weiss, F. Storici, Mispaired rNMPs in DNA are mutagenic and are targets of mismatch repair and RNases H, Nat. Struct. Mol. Biol. 19 (2012) 98–104.

[24] A. Vaisman, J.P. McDonald, D. Huston, W. Kuban, L. Liu, B. Van Houten, R. Woodgate, Removal of misincorporated ribonucleotides from prokaryotic genomes: an unexpected role for nucleotide excision repair, PLoS Genet. 9 (2013), e1003878.

[25] Y. Cai, N.E. Geacintov, S. Broyde, Ribonucleotides as nucleotide excision repair substrates, DNA Repair (Amst) 13 (2014) 55–60.

[26] M.C. Malfatti, S. Balachander, G. Antoniali, K.D. Koh, C. Saint-Pierre, D. Gasparutto, H. Chon, R.J. Crouch, F. Storici, G. Tell, Abasic and oxidized ribonucleotides embedded in DNA are processed by human APE1 and not by RNase H2, Nucleic Acids Res. 45 (2017) 11193–11212.

[27] S.H. Lao-Sirieix, L. Pellegrini, S.D. Bell, The promiscuous primase, Trends Genet. 21 (2005) 568–572.

[28] J.Y. Choi, R.L. Eoff, M.G. Pence, J. Wang, M.V. Martin, E.J. Kim, L.M. Folkmann, F.P. Guengerich, Roles of the four DNA polymerases of the crenarchaeon *Sulfolobus solfataricus* and accessory proteins in DNA replication, J. Biol. Chem. 286 (2011) 31180–31193.

[29] T.R. Beattie, S.D. Bell, Coordination of multiple enzyme activities by a single PCNA in archaeal Okazaki fragment maturation, EMBO J. 31 (2012) 1556–1567.

[30] G. Desogus, S. Onesti, P. Brick, M. Rossi, F.M. Pisani, Identification and characterization of a DNA primase from the hyperthermophilic archaeon *Methanococcus jannaschii*, Nucleic Acids Res. 27 (1999) 4444–4450.

[31] M. Le Breton, G. Henneke, C. Norais, D. Flament, H. Myllykallio, J. Querellou, J.P. Raffin, The heterodimeric primase from the euryarchaeon *Pyrococcus abyssi:* a multifunctional enzyme for initiation and repair? J. Mol. Biol. 374 (2007) 1172–1185.

[32] L. Liu, K. Komori, S. Ishino, A.A. Bocquier, I.K. Cann, D. Kohda, Y. Ishino, The archaeal DNA primase: biochemical characterization of the p41–p46 complex from *Pyrococcus furiosus*, J. Biol. Chem. 276 (2001) 45484–45490.

[33] L. Greenough, Z. Kelman, A.F. Gardner, The roles of family B and D DNA polymerases in *Thermococcus* species 9 degrees N Okazaki fragment maturation, J. Biol. Chem. 290 (2015) 12514–12522.

[34] G. Henneke, *In vitro* reconstitution of RNA primer removal in *Archaea* reveals the existence of two pathways, Biochem. J. 447 (2012) 271–280.

[35] G. Henneke, D. Flament, U. Hubscher, J. Querellou, J.P. Raffin, The hyperthermophilic euryarchaeota *Pyrococcus abyssi* likely requires the two DNA polymerases D and B for DNA replication, J. Mol. Biol. 350 (2005) 53–64.
[36] I.K. Cann, S. Ishino, I. Hayashi, K. Komori, H. Toh, K. Morikawa, Y. Ishino, Functional interactions of a homolog of proliferating cell nuclear antigen with DNA polymerases in *Archaea*, J. Bacteriol. 181 (1999) 6591–6599.
[37] B.R. Berquist, P. Dassarma, S. Dassarma, Essential and non-essential DNA replication genes in the model halophilic archaeon, *Halobacterium* sp. *NRC-1*, BMC Genet. 8 (2007) 31.
[38] L. Cubonova, T. Richardson, B.W. Burkhart, Z. Kelman, B.A. Connolly, J.N. Reeve, T.J. Santangelo, Archaeal DNA polymerase D but not DNA polymerase B is required for genome replication in *Thermococcus kodakarensis*, J. Bacteriol. 195 (2013) 2322–2328.
[39] F. Sarmiento, J. Mrazek, W.B. Whitman, Genome-scale analysis of gene function in the hydrogenotrophic methanogenic archaeon *Methanococcus maripaludis*, Proc. Natl. Acad. Sci. U. S. A. 110 (2013) 4726–4731.
[40] F. Boudsocq, S. Iwai, F. Hanaoka, R. Woodgate, *Sulfolobus solfataricus* P2 DNA polymerase IV (Dpo4): an archaeal DinB-like DNA polymerase with lesion-bypass properties akin to eukaryotic poleta, Nucleic Acids Res. 29 (2001) 4607–4616.
[41] L.J. Lin, A. Yoshinaga, Y. Lin, C. Guzman, Y.H. Chen, S. Mei, A.M. Lagunas, S. Koike, S. Iwai, M.A. Spies, S.K. Nair, R.I. Mackie, Y. Ishino, I.K. Cann, Molecular analyses of an unusual translesion DNA polymerase from *Methanosarcina acetivorans* C2A, J. Mol. Biol. 397 (2010) 13–30.
[42] A. Palud, G. Villani, S. L'Haridon, J. Querellou, J.P. Raffin, G. Henneke, Intrinsic properties of the two replicative DNA polymerases of *Pyrococcus abyssi* in replicating abasic sites: possible role in DNA damage tolerance? Mol. Microbiol. 70 (2008) 746–761.
[43] T.T. Richardson, L. Gilroy, Y. Ishino, B.A. Connolly, G. Henneke, Novel inhibition of archaeal family-D DNA polymerase by uracil, Nucleic Acids Res. 41 (2013) 4207–4218.
[44] J. Abellon-Ruiz, K.J. Waldron, B.A. Connolly, *Archaeoglobus fulgidus* DNA polymerase D: a zinc-binding protein inhibited by hypoxanthine and uracil, J. Mol. Biol. 428 (2016) 2805–2813.
[45] B.A. Connolly, Recognition of deaminated bases by archaeal family-B DNA polymerases, Biochem. Soc. Trans. 37 (2009) 65–68.
[46] T.A. Guilliam, B.A. Keen, N.C. Brissett, A.J. Doherty, Primase-polymerases are a functionally diverse superfamily of replication and repair enzymes, Nucleic Acids Res. 43 (2015) 6651–6664.
[47] G. Erauso, A.L. Reysenbach, A. Godfroy, J.R. Meunier, B. Crump, F. Partensky, J.A. Baross, V. Marteinsson, G. Barbier, N.R. Pace, D. Prieur, *Pyrococcus abyssi* sp. nov., a new hyperthermophilic archaeon isolated from a deep-sea hydrothermal vent, Arch. Microbiol. 160 (1993) 338–349.
[48] H. Myllykallio, P. Lopez, P. Lopez-Garcia, R. Heilig, W. Saurin, Y. Zivanovic, H. Philippe, P. Forterre, Bacterial mode of replication with eukaryotic-like machinery in a hyperthermophilic archaeon, Science 288 (2000) 2212–2215.
[49] B. Castrec, C. Rouillon, G. Henneke, D. Flament, J. Querellou, J.P. Raffin, Binding to PCNA in euryarchaeal DNA replication requires two PIP motifs for DNA polymerase D and one PIP motif for DNA polymerase B, J. Mol. Biol. 394 (2009) 209–218.
[50] C. Rouillon, G. Henneke, D. Flament, J. Querellou, J.P. Raffin, DNA polymerase switching on homotrimeric PCNA at the replication fork of the euryarchaea *Pyrococcus abyssi*, J. Mol. Biol. 369 (2007) 343–355.
[51] J. Gouge, C. Ralec, G. Henneke, M. Delarue, Molecular recognition of canonical and deaminated bases by *P. abyssi* family B DNA polymerase, J. Mol. Biol. 423 (2012) 315–336.
[52] P.F. Pluchon, T. Fouqueau, C. Creze, S. Laurent, J. Briffotaux, G. Hogrel, A. Palud, G. Henneke, A. Godfroy, W. Hausner, M. Thomm, J. Nicolas, D. Flament, An extended network of genomic maintenance in the archaeon *Pyrococcus abyssi* highlights unexpected associations between eucaryotic homologs, PLoS One 8 (2013), e79707.
[53] C. Ralec, E. Henry, M. Lemor, T. Killelea, G. Henneke, Calcium-driven DNA synthesis by a high-fidelity DNA polymerase, Nucleic Acids Res. 45 (2017) 12425–12440.
[54] M.S. Tang, V.A. Bohr, X.S. Zhang, J. Pierce, P.C. Hanawalt, Quantification of aminofluorene adduct formation and repair in defined DNA sequences in mammalian cells using the UVRABC nuclease, J. Biol. Chem. 264 (1989) 14455–14462.
[55] W. Ginoza, C.J. Hoelle, K.B. Vessey, C. Carmack, Mechanisms of inactivation of single-stranded virus nucleic acids by heat, Nature 203 (1964) 606–609.
[56] S. Gon, R. Napolitano, W. Rocha, S. Coulon, R.P. Fuchs, Increase in dNTP pool size during the DNA damage response plays a key role in spontaneous and induced-mutagenesis in *Escherichia coli*, Proc. Natl. Acad. Sci. U. S. A. 108 (2011) 19311–19316.
[57] L.J. Wheeler, C.K. Mathews, Nucleoside triphosphate pool asymmetry in mammalian mitochondria, J. Biol. Chem. 286 (2011) 16992–16996.
[58] M.F. White, Archaeal DNA repair: paradigms and puzzles, Biochem. Soc. Trans. 31 (2003) 690–693.
[59] E. Crespan, A. Furrer, M. Rosinger, F. Bertoletti, E. Mentegari, G. Chiapparini, R. Imhof, N. Ziegler, S.J. Sturla, U. Hubscher, B. van Loon, G. Maga, Impact of ribonucleotide incorporation by DNA polymerases beta and lambda on oxidative base excision repair, Nat. Commun. 7 (2016), 10805.
[60] A.F. Moon, J.M. Pryor, D.A. Ramsden, T.A. Kunkel, K. Bebenek, L.C. Pedersen, Structural accommodation of ribonucleotide incorporation by the DNA repair enzyme polymerase Mu, Nucleic Acids Res. 45 (2017) 9138–9148.
[61] H. Ordonez, M.L. Uson, S. Shuman, Characterization of three mycobacterial DinB (DNA polymerase IV) paralogs highlights DinB2 as naturally adept at ribonucleotide incorporation, Nucleic Acids Res. 42 (2014) 11056–11070.
[62] M.A. Reijns, B. Rabe, R.E. Rigby, P. Mill, K.R. Astell, L.A. Lettice, S. Boyle, A. Leitch, M. Keighren, F. Kilanowski, P.S. Devenney, D. Sexton, G. Grimes, I.J. Holt, R.E. Hill, M.S. Taylor, K.A. Lawson, J.R. Dorin, A.P. Jackson, Enzymatic removal of ribonucleotides from DNA is essential for mammalian genome integrity and development, Cell 149 (2012) 1008–1022.
[63] L. Sauguet, P. Raia, G. Henneke, M. Delarue, Shared active site architecture between archaeal PolD and multi-subunit RNA polymerases revealed by X-ray crystallography, Nat. Commun. 7 (2016), 12227.
[64] C. Cozens, V.B. Pinheiro, A. Vaisman, R. Woodgate, P. Holliger, A short adaptive path from DNA to RNA polymerases, Proc. Natl. Acad. Sci. U. S. A. 109 (2012) 8067–8072.
[65] O. Rechkoblit, Y.K. Gupta, R. Malik, K.R. Rajashankar, R.E. Johnson, L. Prakash, S. Prakash, A.K. Aggarwal, Structure and mechanism of human PrimPol, a DNA polymerase with primase activity, Sci. Adv. 2 (2016), e1601317.

[66] S. Ishino, Y. Nishi, S. Oda, T. Uemori, T. Sagara, N. Takatsu, T. Yamagami, T. Shirai, Y. Ishino, Identification of a mismatch-specific endonuclease in hyperthermophilic *Archaea*, Nucleic Acids Res. 44 (2016) 2977–2986.
[67] M. van Wolferen, M. Ajon, A.J. Driessen, S.V. Albers, How hyperthermophiles adapt to change their lives: DNA exchange in extreme conditions, Extremophiles 17 (2013) 545–563.
[68] M. Ajon, S. Frols, M. van Wolferen, K. Stoecker, D. Teichmann, A.J. Driessen, D.W. Grogan, S.V. Albers, C. Schleper, UV-inducible DNA exchange in hyperthermophilic *Archaea* mediated by type IV pili, Mol. Microbiol. 82 (2011) 807–817.
[69] A. Godfroy, A. Postec, N. Raven, Growth of hyperthermophilic microorganisms for physiological and nutritional studies, Extremophiles 35 (2006) 93–108.
[70] A. Godfroy, N.D. Raven, R.J. Sharp, Physiology and continuous culture of the hyperthermophilic deep-sea vent archaeon *Pyrococcus abyssi* ST549, FEMS Microbiol. Lett. 186 (2000) 127–132.
[71] Z. Kong, S. Jia, A.L. Chabes, P. Appelblad, R. Lundmark, T. Moritz, A. Chabes, Simultaneous determination of ribonucleoside and deoxyribonucleoside triphosphates in biological samples by hydrophilic interaction liquid chromatography coupled with tandem mass spectrometry, Nucleic Acids Res. 46 (2018) e66.
[72] L. Meslet-Cladiere, C. Norais, J. Kuhn, J. Briffotaux, J.W. Sloostra, E. Ferrari, U. Hubscher, D. Flament, H. Myllykallio, A novel proteomic approach identifies new interaction partners for proliferating cell nuclear antigen, J. Mol. Biol. 372 (2007) 1137–1148.
[73] G. Henneke, Y. Gueguen, D. Flament, P. Azam, J. Querellou, J. Dietrich, U. Hubscher, J.P. Raffin, Replication factor C from the hyperthermophilic archaeon *Pyrococcus abyssi* does not need ATP hydrolysis for clamp-loading and contains a functionally conserved RFC PCNA-binding domain, J. Mol. Biol. 323 (2002) 795–810.